The Canadian Mineralogist
Vol. 32, pp. 575-587 (1994)

LREE-RICH NIOBIAN TITANITE FROM MOUNT BISSON, BRITISH COLUMBIA: CHEMISTRY AND EXCHANGE MECHANISMS

JAMES K. RUSSELL, LEE A. GROAT AND ARTHUR A.D. HALLERAN*

Department of Geological Sciences, The University of British Columbia, Vancouver, British Columbia V6T 1Z4

ABSTRACT

Niobian titanite enriched in light rare-earth elements (*LREE*) occurs in allanite-bearing granitic pegmatite associated with alkaline igneous and metasomatic rocks within metamorphic gneisses and amphibolites at Mount Bisson, near MacKenzie, British Columbia. The titanite is compositionally zoned, commonly intergrown with accessory allanite, apatite, ilmenite, zircon and thorite, and found in a rock with 555 ppm Nb. It differs from reported cases of niobian titanite in having up to 3.5 wt. % *LREE* and Y, and no detectable Ta. Titanite found in other rock-types at Mount Bisson contains various amounts of *LREE*+Y, but little Nb. Compared to niobian titanite from elsewhere, the Mount Bisson samples have intermediate contents of Nb and higher abundances of *LREE*. Three mechanisms of substitution seem consistent with our compositional data: (i) $[Nb, Ta]^{5+} + [^{VI}Al, Fe^{3+}] \rightarrow 2Ti^{4+}$, (ii) $[^{VI}Al, Fe^{3+}] + [OH]^{-} \rightarrow Ti^{4+} + O^{2-}$, and (iii) $[LREE, Y]^{3+} + [^{VI}Al, Fe^{3+}] \rightarrow Ca^{2+} + Ti^{4+}$. Chondrite-normalized (cn) patterns show that most titanite samples have the same degree of *LREE* enrichment, and a greater degree of enrichment in *LREE*, except for La, than the host rock. Titanite samples from different rock-types commonly show broadly similar *LREE* patterns, although titanite originating from alkaline systems (*e.g.*, fenites or intrusive rocks) is characterized by moderate to high negative values of $[Ce/La]_{cn}$. In contrast, preliminary data from subalkaline intrusions suggest values of $[Ce/La]_{cn}$ near zero. These differences in patterns probably reflect the presence or absence of other *REE*-rich accessory phases rather than the *REE* content of the system. Although many of the samples of titanite are compositionally zoned in terms of *LREE* and Nb concentrations, no systematic variations were found in REE_{cn} patterns between or within grains.

Keywords: titanite, composition, niobium, rare-earth elements, igneous, metasomatic, fenite, Mount Bisson, British Columbia.

SOMMAIRE

Nous avons trouvé de la titanite niobifère enrichie en terres rares légères (*TRL*) dans une pegmatite granitique à quartz + allanite associée aux roches ignées et métasomatiques mises en place dans les gneiss métamorphiques et les amphibolites au Mont Bisson, en Colombie-Britannique. La titanite est zonée, montre une association à allanite, apatite, ilménite, zircon et thorite, et se trouve dans une roche qui contient 555 ppm Nb. Cet exemple de titanite niobifère diffère des autres dans la littérature par sa teneur élevée en *TRL* (3.5% par poids) et en Y, et par l'absence de Ta. La titanite des autres types de roche au Mont Bisson contient des teneurs variées en *TRL* et en Y, mais sans Nb. Par contre, en comparaison des exemples connus de titanite niobifère, nos échantillons ont des teneurs intermédiaires de Nb et des teneurs plus élevées en terres rares légères. Trois mécanismes de substitution semblent expliquer nos données: (i) $[Nb,Ta]^{5+} + [^{VI}Al,Fe^{3+}] \rightarrow 2Ti^{4+}$, (ii) $[^{VI}Al,Fe^{3+}] + [OH]^{-} \rightarrow Ti^{4+} + O^{2-}$, et (iii) $[TRL,Y]^{3+} + [^{VI}Al,Fe^{3+}] \rightarrow Ca^{2+} + Ti^{4+}$. Une comparaison des spectres de concentrations de terres rares normalisées par rapport aux abondances chondritiques montre que la plupart de nos échantillons de titanite possèdent un degré comparable d'enrichissement en terres rares, et un enrichissement plus marqué en *TRL*, sauf pour le La, que les roches hôtes. Les échantillons des diverses lithologies montrent un spectre sembable dans la région des *TRL*, quoique dans les roches hôte alcalines (fénites, roches intrusives), le rapport [Ce/La] des concentrations normalisées peut être fortement négatif. Par contre, nos données préliminaires indiquent que dans les roches intrusives subalcalines, ce même rapport est sensiblement zéro. Les différences dépendent probablement plus de la présence ou l'absence d'autres phases accessoires que de la quantité des terres rares dans le système. Quoique plusieurs cristaux étudiés sont zonés en termes des concentrations de *TRL* et de Nb, nous n'avons pas trouvé de variations systématiques à l'intérieur des grains ou d'un grain à un autre.

(Traduit par la Rédaction)

Mots-clés: titanite, composition, niobium, terres rares, roche ignée, roche métasomatique, fénite, mont Brisson, Colombie-Britannique.

* Present address: Department of Geology and Geophysics, The University of Calgary, Calgary, Alberta T2N 1N4.

INTRODUCTION

Niobium-rich varieties of titanite have previously been described by Clark (1974), Paul *et al.* (1981), Groat *et al.* (1985) and Hawthorne *et al.* (1991). These samples also contain substantial tantalum (3.7 to 16.0 wt.% Ta_2O_5), but commonly lack significant quantities of rare-earth elements (*REE*). Titanite enriched in light rare-earth elements (*LREE*) and Y occurs fairly commonly in nature and has been important in petrogenetic studies (*e.g.*, Exley 1980, Sawka *et al.* 1984, Nakada 1991), but none containing substantial Nb has been reported.

Titanite containing substantial amounts of *LREE* and Y is present in a variety of igneous and metasomatic rock-types from the Mount Bisson area of British Columbia. In addition, one of the pegmatite bodies is characterized by titanite enriched in Nb as well as *LREE* and Y but, in contrast to examples from the literature, without detectable Ta. Table 1 summarizes the mineralogical and chemical characteristics of the Mount Bisson rocks from which titanite has been analyzed. In this paper, we present chemical data for these apparently unique compositions of titanite, and compare them to other *LREE*-enriched samples of titanite from Mount Bisson, as well as to niobian titanite from the literature. The Mount Bisson data, combined with the data in the literature, provide a database from which can be inferred possible mechanisms of substitution involved in the accommodation of significant amounts of pentavalent and trivalent cations, and their relative importance. The *REE* data also are used qualitatively to examine aspects of *LREE* partitioning in titanite-bearing mineral assemblages derived from igneous and metasomatic rock-types.

GEOLOGICAL SETTING

At Mount Bisson, situated in the Wolverine Mountain Range 64 km northwest of the town of MacKenzie and 10 km southwest of Williston Lake, a diverse suite of igneous rocks (Halleran & Russell 1990, 1993) intrudes Proterozoic and younger metamorphic gneisses, schists and amphibolites of the Wolverine metamorphic complex (Ferri & Melville 1988, Deville & Struik 1990). The term "Wolverine metamorphic complex" refers to rocks of the Ingenika Group (*e.g.*, Mansy & Gabrielse 1978) which, through regional metamorphism and deformation, have had their original composition, mineralogy and structure obliterated. Subsequently, these metamorphic rocks have been extensively intruded by several generations of felsic magma and associated pegmatites (Tipper *et al.* 1974, Parrish 1979, Ferri & Melville 1988, 1989). The intrusive rocks occur as small, irregularly shaped stocks, dykes and sills and have a varied mineralogy (Table 1). Most intrusions consist of quartz-bearing, subalkaline granitic pegmatite; however, there is a volumetrically subordinate suite of *REE*-enriched, alkaline intrusions. The latter intrusive suite cross-cuts all major metamorphic fabrics and structures in rocks of the Wolverine metamorphic complex. Many of the older metamorphic and igneous rocks that are adjacent to these alkaline plutonic rocks seem to have been metasomatically modified (fenitized). They have been texturally, mineralogically and chemically altered and share several traits: i) they show evidence of partial replacement of original minerals and obliteration of primary textures or metamorphic fabric, ii) they contain modal aegirine-augite as an important ferromagnesian phase (Table 1), iii) with increasing degree of metasomatism, K-feldspar, allanite, titanite and apatite increase in modal abundance, and iv) the rocks have elevated concentrations of total alkalis and *REE* (1750–4500 ppm: Table 1).

The alkaline intrusions (samples 23, 7911; Table 1) and the fenitized rocks show a similar degree of *LREE* enrichment and contain significant modal *REE*-bearing accessories such as allanite, apatite and titanite. The metasomatic event is most evident in

TABLE 1. MINERALOGICAL AND CHEMICAL ATTRIBUTES OF THE MOUNT BISSON ROCK TYPES

Labels	Rock Type	ΣREE (ppm)	Nb(ppm)	Qtz	Kfs/Pl	Agt/Aug	Hbl	Aln	Ttn	Ap	Other
				Intrusive Rocks							
7835	hornblende pegmatite	607	13	2	77	0	20	tr	tr	tr	0
7819	quartz syenite	290	22	2	88	10	0	0	tr	tr	0
23	aegirine-augite syenite	1366	150	0	58	40*	0	tr	2	tr	0
7911	allanite pegmatite	>29,090	241	tr	70	15*	0	10	tr	2	Zrn
				Metasomatically Modified Rocks							
7842	Aln-bearing pegmatite	4498	555	28	64	2*	0	3	2	1	Zrn, Th
7803	monzonite	1751	118	tr	89	10**	0	0	1	tr	Zrn
7837	fenitized gneiss/amphibolite	3090	35	tr	90	9	tr	0	0.5	0.5	Zrn
7823	fenitized gneiss/amphibolite	3325	34	tr	79	20*	tr	0.5	0.5	tr	Zrn

Mineral abbreviations are after Kretz (1983); * and ** denote aegirine augite or aegirine augite overgrowths, respectively.

metamorphic gneisses and amphibolites where, locally at least, the metasomatism completely overprints the original mineralogy and obliterates metamorphic fabrics. Less pronounced effects of metasomatism are seen in a number of the older subalkaline intrusive bodies, where a rim of aegirine-augite is found as an overgrowth on older igneous augite (sample 7803, Table 1). Field relationships, combined with the above mineralogical and chemical observations, suggest that the metasomatic fluids causing fenitization derive from the alkaline intrusions (Halleran 1991).

Titanite found in the fenites and most Mount Bisson igneous rocks is generally *LREE*-enriched, although there is significant chemical variation among titanite separates from different rock-types. In most cases, the titanite lacks Nb. The single occurrence of *LREE*-rich niobian titanite occurs in an allanite-bearing granitic pegmatite body that predates, and has been partly affected by, the metasomatic event. This pegmatite contains 555 ppm Nb (sample 7842; Table 1), although the rock and the titanite have no appreciable Ta.

Petrology

The allanite-bearing granitic pegmatite in question is characterized by a strong foliation and by distinct mineralogical banding comprised of aggregates of mafic minerals. Sample 7842 contains (in order of decreasing abundance) K-feldspar, quartz, minor green pleochroic aegirine-augite, plagioclase, and accessory allanite, titanite, apatite, Nb-bearing ilmenite, pink pleochroic zircon and thorite (Fig. 1).

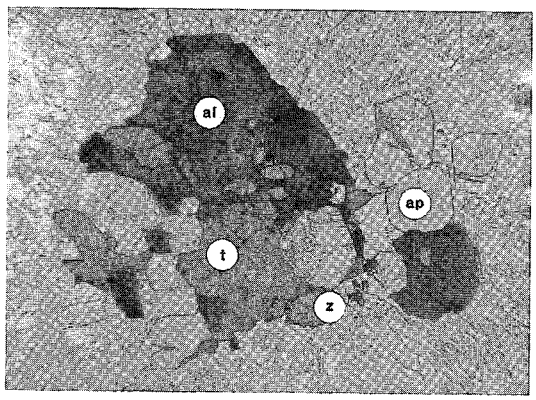

FIG. 1. Transmitted-light photograph of petrographic relationships in pegmatite 7842 showing intergrowth of allanite (al), titanite (t), apatite (ap), zircon (z) and ilmenite inclusions in a groundmass of quartz and K-feldspar. Width of field of view: 2.4 mm.

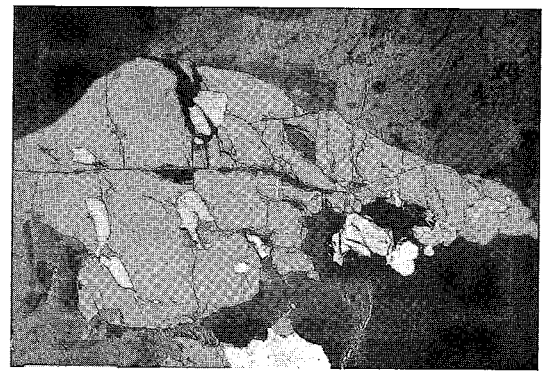

FIG. 2. Back-scattered electron image of sample 7842 showing one of the *LREE*-enriched, niobian titanite crystals (grey) with inclusions of niobium-bearing ilmenite (bright white). Width of field of view: 1 mm.

Polycrystalline grains of quartz are elongate and parallel the mineralogical banding. Apatite occurs as well-formed subhedral to euhedral crystals and is commonly enclosed by anhedral to subhedral allanite. Allanite and apatite both show oscillatory zoning, although the margin of allanite grains more commonly shows patchy zoning. On the basis of textural features, allanite appears to be late-formed relative to apatite. Titanite occurs as light brown-grey pleochroic, anhedral to subhedral crystals, 0.4–1.2 mm across. It is commonly enclosed by sheets of anhedral allanite and intergrown with apatite (Fig. 1). Relative to allanite, titanite appears also to be a relatively early-formed phase. Niobium-bearing ilmenite occurs as inclusions in the titanite (Fig. 2). Thorite and zircon also occur intergrown with titanite.

Chemical data for sample 7842 (Table 2) show that it is a quartz-normative, subalkaline granitic rock. The pegmatite contains high concentrations of ΣREE, Nb,

TABLE 2. CHEMICAL COMPOSITION OF FENITIZED ALLANITE-BEARING GRANITIC PEGMATITE SAMPLE 7842

Oxide	Wt. %	Element	ppm	Element	ppm	Index	Value
SiO_2	71.50	Rb	63	La	1240	$[La/Lu]_n$	929.6
TiO_2	1.17	Sr	1031	Ce	2440	$[La/Sm]_n$	9.2
Al_2O_3	12.43	Ba	5291	Pr	240	$[Tb/Yb]_n$	17.6
Fe_2O_3	0.84	Sc	7.6	Nd	430	[Eu/Sm]	0.23
FeO	1.43	Y	138	Sm	77		
MnO	0.09	Zr	245	Eu	18		
MgO	0.51	Nb	555	Tb	6		
CaO	2.46	Th	1910	Dy	33		
Na_2O	2.86	U	93	Ho	4		
K_2O	5.86			Yb	1.7		
P_2O_5	0.14			Lu	0.15		
Total	99.30						
LOI	0.34						

LOI (loss on ignition) was performed prior to XRF analysis for major, minor and trace elements. Rare earth elements, Sc, Th, and U concentrations were sought by neutron activation analysis.

La, Ce, and Pr. Also reported in Table 2 are the calculated indices of total, light and heavy *REE* fractionation, $[La/Lu]_{cn}$, $[La/Sm]_{cn}$ and $[Tb/Yb]_{cn}$, respectively. The pegmatite shows significant *REE* fractionation, which has affected the *HREE* more than the *LREE*.

Field relationships and textures indicate that the allanite-bearing granitic pegmatite predates both the last regional deformational event and the later metasomatism that modified rocks within the Wolverine metamorphic complex. There are several other lines of evidence suggesting that this pegmatite is, in part, a product of metasomatism. Firstly, aegirine-augite is the principal ferromagnesian phase in the pegmatite, although the rock is chemically subalkaline. Secondly, the rock contains abundant *LREE*-enriched accessory allanite, titanite and apatite. In terms of total *REE* content, the chemical composition of the pegmatite closely parallels that of several fenitized gneisses and amphibolites (*cf.* Figs. 6a, c). It is possible, therefore, that the titanite is not simply a product of igneous crystallization, but results from metasomatic processes. The secondary nature of such titanite is similar to that proposed for the examples of Nb–Ta titanite described by Paul *et al.* (1981) and Groat *et al.* (1985).

Experimental

Mineral compositions were measured using the automated Cameca SX–50 electron microprobe at the Department of Geological Sciences, University of British Columbia. Operating conditions for wavelength-dispersion analysis included: specimen current 30 nA, excitation voltage 20 kV, a 5–10 μm beam diameter, and sample collection times of 20 seconds for Si, Al, Ti, Mn, Fe, Mg, Ca, Na and Sr, and 40 seconds for La, Ce, Pr, Nd, Sm, Y, Ta and Nb. The elements Ta, Sr, Mn, Mg and, commonly, Na were found to be at or below detection limits: estimated limits of detection, in wt.% oxide, were >0.20, 0.10, 0.14, 0.06 and 0.10, respectively. For several titanite samples, wavelength-dispersion scans were run at higher currents to search for detectable concentrations of Ho, Gd, and Dy, but none was found.

Additional experimental conditions and the standards used in the measurement of titanite compositions are given in Table 3. Peak and background positions used in the measurement of La, Ce, Pr, Nd, Sm, Y and Nb concentrations were chosen after running full wavelength-dispersion scans at specimen currents of 40–100 nA on both calibration standards and on unknown mineral specimens. This procedure was used to avoid potential peak-overlap problems. Analysis points were selected on the basis of reconnaissance back-scattered electron images (BSE) and energy-dispersion spectra (EDS).

Twenty-one measured compositions of grains of *LREE*-rich niobian titanite from pegmatite sample 7842 are reported in Table 4. Also reported are the mean analytical uncertainties (wt. %) for each oxide measured. Structural formulae (Table 4) have been normalized on the basis of three cations using the Turbo-Pascal computer program Form1 (Mader *et al.* 1988). In addition, the mean analytical uncertainties on the oxide concentrations have been propagated through the mineral formulae calculations (Table 4) to give mean uncertainties on the cations. The propagated uncertainties in cations per formula unit (pfu) are represented as 2σ error bars in Figures 3 and 4. Representative compositions of individual grains of niobium-bearing ilmenite from the same sample are reported in Table 5.

TABLE 3. EXPERIMENTAL CONDITIONS AND STANDARDS USED IN ELECTRON–MICROPROBE ANALYSIS OF TITANITE

Element	Crystal	X-ray Line	Analytical Precision (%) on Oxide	Standard
Si	TAP	$K\alpha_1$	0.2	Diopside
Al	TAP	$K\alpha_1$	0.2	Garnet
Ti	PET	$K\alpha_1$	0.1	Rutile
Mn	LiF	$K\alpha_1$	0.2	Pyroxmangite
Fe	LiF	$K\alpha_1$	0.2	Fayalite
Mg	TAP	$K\alpha_1$	0.2	Forsterite
Ca	PET	$K\alpha_1$	0.3	Diospide
Na	TAP	$K\alpha_1$	0.5	Aegirine-Augite
Sr	PET	$L\alpha_1$	0.2	Strontianite
Y	TAP	$L\alpha_1$	0.6	Glass S261
Nb	PET	$L\alpha_1$	1.4	Microlite
La	PET	$L\alpha_1$	0.7	Glass S261
Ce	PET	$L\alpha_1$	0.7	Glass S261
Pr	PET	$L\beta_1$	0.8	Glass S261
Nd	LiF	$L\beta_1$	0.8	Glass S260
Sm	LiF	$L\beta_1$	1.4	Glass S260

Standards S260 and S261 are REE-doped glasses of Drake and Weill (1972).

Crystal Chemistry and Schemes of Substitution

The compositions of titanite in the Mount Bisson suite are treated as two distinct groups in the following discussion. The first group includes only the *LREE*-rich niobian titanite found in the allanite-bearing granitic pegmatite (7842). The second group is made up of *LREE*-enriched titanite from a variety of other rock-types (Table 1). These data, combined with data from the literature, are used to study the mechanisms that facilitate extensive substitution of pentavalent and trivalent cations for Ti.

The titanite in sample 7842 is chemically zoned and shows significant variation in Nb, Ti, ^{VI}Al, Fe^{3+}, $\Sigma LREE$ and Y, although core-to-rim variations are neither systematic nor consistent among grains. The titanite from the other Mount Bisson rocks shows greater variation in Ca, $\Sigma LREE$ and Y, and less variation in Ti, ^{VI}Al, Fe^{3+} and Nb. Compared to Nb–Ta-bearing titanite from the literature (*e.g.*, Clark 1974, Paul *et al.* 1981, Fleet & Henderson 1985, Groat *et al.*

TABLE 4. ELECTRON-MICROPROBE DATA (wt.%) ON LREE-BEARING NIOBIAN TITANITE FROM SAMPLE 7842

Oxide	783-1	783-1B	783-2	783-3	783-4	783-5	784-1	784-2	784-3	785-1	785-2
SiO_2	29.03	29.08	29.01	29.13	28.97	29.41	28.98	28.95	29.21	29.15	28.85
Al_2O_3	1.15	1.18	1.48	1.17	1.63	1.11	1.20	0.76	1.24	1.27	1.17
TiO_2	33.11	32.93	32.77	32.60	32.80	33.81	34.05	34.90	33.69	33.15	33.19
Fe_2O_3	2.72	2.73	1.95	2.82	1.95	2.44	2.17	2.27	2.13	2.42	2.27
CaO	25.93	25.96	26.21	26.32	26.23	26.99	26.20	25.93	26.04	25.76	25.88
La_2O_3	0.08	0.10	0.01	0.01	0.02	0.02	0.07	0.19	0.05	0.09	0.06
Ce_2O_3	0.90	0.87	0.45	0.43	0.55	0.41	0.73	1.17	0.65	0.84	0.74
Pr_2O_3	0.13	0.13	0.06	0.09	0.02	0.09	0.17	0.25	0.12	0.19	0.17
Nd_2O_3	0.64	0.77	0.44	0.49	0.52	0.49	0.57	0.69	0.55	0.65	0.58
Sm_2O_3	0.19	0.16	0.12	0.09	0.19	0.11	0.11	0.08	0.16	0.11	0.13
Y_2O_3	0.36	0.38	0.68	0.67	0.61	0.14	0.30	0.28	0.34	0.41	0.41
Nb_2O_5	3.22	3.22	3.85	3.62	3.12	2.20	2.98	1.51	2.49	2.57	2.81
Total	97.46	97.51	97.03	97.44	96.61	97.22	97.53	96.98	96.67	96.61	96.26
					Calculated on the basis of 3 cations						
Si	0.9958	0.9971	0.9953	0.9960	0.9952	0.9984	0.9901	0.9951	1.0030	1.0045	0.9980
^{IV}Al	0.0042	0.0029	0.0047	0.0040	0.0048	0.0016	0.0099	0.0049	0.0000	0.0000	0.0020
Σ	1.0000	1.0000	1.0000	1.0000	1.0000	1.0000	1.0000	1.0000	1.0030	1.0045	1.0000
^{VI}Al	0.0422	0.0448	0.0552	0.0432	0.0612	0.0428	0.0384	0.0259	0.0502	0.0516	0.0457
Ti	0.8541	0.8491	0.8455	0.8382	0.8473	0.8632	0.8748	0.9021	0.8700	0.8591	0.8634
Fe^{3+}	0.0702	0.0704	0.0503	0.0726	0.0504	0.0623	0.0558	0.0587	0.0550	0.0628	0.0591
Nb	0.0499	0.0499	0.0597	0.0560	0.0485	0.0338	0.0460	0.0235	0.0387	0.0400	0.0439
Σ	1.0165	1.0142	1.0108	1.0099	1.0074	1.0021	1.0151	1.0102	1.0138	1.0134	1.0122
Ca	0.9530	0.9537	0.9635	0.9642	0.9654	0.9817	0.9591	0.9550	0.9580	0.9511	0.9592
La	0.0010	0.0013	0.0001	0.0001	0.0003	0.0003	0.0009	0.0024	0.0006	0.0011	0.0008
Ce	0.0113	0.0109	0.0057	0.0054	0.0069	0.0051	0.0091	0.0147	0.0082	0.0106	0.0094
Pr	0.0016	0.0016	0.0008	0.0011	0.0003	0.0011	0.0021	0.0031	0.0015	0.0024	0.0021
Nd	0.0078	0.0094	0.0054	0.0060	0.0064	0.0059	0.0070	0.0085	0.0067	0.0080	0.0072
Sm	0.0022	0.0019	0.0014	0.0011	0.0022	0.0013	0.0013	0.0009	0.0019	0.0013	0.0015
Y	0.0066	0.0069	0.0124	0.0122	0.0112	0.0025	0.0055	0.0051	0.0062	0.0075	0.0075
Σ	0.9835	0.9858	0.9892	0.9901	0.9926	0.9979	0.9849	0.9898	0.9832	0.9820	0.9878

Oxide	785-3	785-4	785-5	785-6	785-7	7842-1	7842-9	10-A	11A	12A	Ave 1σ
SiO_2	28.79	29.33	29.37	28.63	29.31	27.87	29.09	28.18	28.88	28.68	0.18
Na_2O	b.d.	b.d.	b.d.	b.d.	b.d.	0.29	b.d.	b.d.	0.14	b.d.	0.12
Al_2O_3	1.06	1.13	1.41	0.88	1.23	1.66	1.31	0.65	1.36	0.74	0.06
TiO2	32.85	33.95	32.99	33.51	33.82	30.25	31.89	33.52	30.64	33.43	0.34
Fe_2O_3	3.04	1.18	2.38	2.84	2.21	2.68	2.73	2.82	3.03	2.94	0.21
CaO	25.31	26.20	26.15	25.73	26.54	25.58	25.77	25.52	26.39	25.73	0.10
La_2O_3	0.14	0.04	0.02	0.15	0.03	0.11	0.10	0.33	b.d.	0.27	0.04
Ce_2O_3	1.10	0.69	0.57	1.17	0.56	0.74	0.66	1.44	0.40	1.43	0.04
Pr_2O_3	0.13	0.14	0.07	0.20	0.13	0.19	0.05	0.18	0.05	0.14	0.22
Nd_2O_3	0.93	0.55	0.53	0.95	0.40	0.72	0.50	0.96	0.23	0.87	0.21
Sm_2O_3	0.27	0.15	0.17	0.21	0.07	0.05	0.16	0.19	0.07	0.05	0.05
Y_2O_3	0.42	0.39	0.47	0.30	0.29	0.43	0.78	0.40	0.34	0.38	0.10
Nb_2O_5	2.47	2.31	3.41	2.83	2.46	5.65	3.70	2.17	5.38	2.31	0.10
Total	96.51	96.06	97.54	97.40	97.05	96.22	96.74	96.36	96.91	96.97	
					Calculated on the basis of 3 cations						
Si	0.9995	1.0117	1.0020	0.9875	0.9993	0.9722	1.0043	0.9838	0.9932	0.9922	0.0081
^{IV}Al	0.0005	0.0000	0.0000	0.0125	0.0007	0.0278	0.0000	0.0162	0.0068	0.0078	0.0002
Σ	1.0000	1.0117	1.0020	1.0000	1.0000	1.0000	1.0043	1.0000	1.0000	1.0000	0.0081
^{VI}Al	0.0428	0.0459	0.0567	0.0233	0.0488	0.0405	0.0533	0.0105	0.0483	0.0223	0.0022
Ti	0.8576	0.8807	0.8464	0.8692	0.8672	0.7936	0.8279	0.8800	0.7924	0.8697	0.0099
Fe^{3+}	0.0794	0.0306	0.0611	0.0737	0.0567	0.0704	0.0709	0.0741	0.0784	0.0765	0.0054
Nb	0.0388	0.0360	0.0526	0.0441	0.0379	0.0891	0.0577	0.0342	0.0836	0.0361	0.0016
Σ	1.0186	0.9933	1.0168	1.0103	1.0105	0.9935	1.0099	0.9988	1.0028	1.0047	0.0116
Ca	0.9414	0.9683	0.9559	0.9508	0.9695	0.9561	0.9532	0.9545	0.9724	0.9537	0.0063
Na	—	—	—	—	—	0.0196	—	—	0.0093	—	0.0080
La	0.0018	0.0005	0.0003	0.0019	0.0004	0.0014	0.0013	0.0042	—	0.0034	0.0005
Ce	0.0140	0.0087	0.0071	0.0148	0.0070	0.0095	0.0083	0.0184	0.0050	0.0181	0.0005
Pr	0.0016	0.0018	0.0009	0.0025	0.0016	0.0024	0.0006	0.0023	0.0006	0.0018	0.0028
Nd	0.0115	0.0068	0.0065	0.0117	0.0049	0.0090	0.0062	0.0120	0.0028	0.0107	0.0026
Sm	0.0032	0.0018	0.0020	0.0025	0.0008	0.0006	0.0019	0.0023	0.0008	0.0006	0.0006
Y	0.0078	0.0072	0.0085	0.0055	0.0053	0.0080	0.0143	0.0074	0.0062	0.0070	0.0018
Σ	0.9814	0.9950	0.9811	0.9897	0.9895	1.0065	0.9858	1.0012	0.9972	0.9953	0.0110

Elements below or at detection (b.d.) include Ta, F, Sr, Mn, Na and Mg and the HREE's Ho, Gd, and Dy.

TABLE 5. REPRESENTATIVE CHEMICAL COMPOSITION OF NIOBIAN ILMENITE FROM SAMPLE 7842

TiO_2 (wt.%)	47.17	49.51	48.63
Nb_2O_5	2.56	1.08	1.44
Ta_2O_5	0.04	b.d.	0.05
Fe_2O_3*	3.87	2.15	3.53
FeO	41.30	42.08	42.13
MgO	0.10	0.09	0.09
MnO	3.75	3.60	3.57
CaO	0.15	0.07	0.01
Total	101.54	99.66	100.94
Calculated on the basis of 12 atoms of oxygen			
Ti	3.732	3.873	3.810
Fe^{3+}	0.153	0.084	0.138
Nb	0.122	0.051	0.068
Ta	0.001	0.000	0.001
Σ	4.008	4.008	4.017
Fe^{2+}	3.633	3.661	3.670
Mg	0.016	0.014	0.014
Mn	0.334	0.317	0.315
Ca	0.017	0.008	0.001

Fe^{3+} is calculated from measured FeO(T). Elements found to be below detection (b.d.) include La, Ce, Pr, Nd, Sm, Ho, Gd and Dy.

1985), the titanite in sample 7842 contains equally high Nb contents, but lacks Ta. Similarly, inclusions of Nb-bearing ilmenite 50–200 μm in size within grains of titanite from sample 7842 have no detectable Ta (Table 5). The Nb-bearing ilmenite occurs only as inclusions within titanite; no other Nb-bearing phases are present.

The structure of titanite was solved by Zachariasen (1930) and refined by Mongiorgi & Riva de Sanseverino (1968). Both studies used the space group *C2/c* (or a symmetrical equivalent) and showed that the dominant structural units are chains of corner-sharing YO_6 (Ti) octahedra running parallel to the *c* axis. These are cross-linked by SiO_4 tetrahedra, producing a $[YOSiO_4]^{2-}$ framework with large cavities enclosing *X* (Ca) atoms in irregular 7-coordinated polyhedra.

Clark (1974), Paul *et al.* (1981) and Groat *et al.* (1985) have suggested several mechanisms of substitution whereby pentavalent cations are accommodated into the titanite structure. These are:

(i) $[Nb, Ta]^{5+} + [^{VI}Al, Fe^{3+}] \rightleftharpoons 2Ti^{4+}$, and

(ii) $[^{VI}Al, Fe^{3+}] + [OH]^{-} \rightleftharpoons Ti^{4+} + O^{2-}$.

Both are coupled substitutions involving the octahedrally coordinated atom in the structure and assume that the *X* (Ca) site contains one Ca atom per formula unit. This is reasonable, given that previous analyses of tantalian–niobian titanite have shown approximately 0.98 – 1.0 Ca atoms pfu (*e.g.*, Clark 1974, Paul *et al.* 1981, Groat *et al.* 1985).

A third mechanism of substitution accommodates the trivalent *LREE* and Y cations in the niobian titanite from Mount Bisson. This is:

(iii) $[LREE, Y]^{3+} + [^{VI}Al, Fe^{3+}] \rightleftharpoons Ca^{2+} + Ti^{4+}$.

Substitution (iii) is the only one that involves cation substitution at both the *X* (Ca) and *Y* (Ti) sites. Note that all three mechanisms require the substitution of trivalent cations for Ti at the octahedral site.

The first mechanism of substitution (i) is represented graphically in Figure 3a, in which Ti is plotted *versus* $^{VI}Al + Fe^{3+} + Nb + Ta + Zr + Sn$. Titanite compositions from Mount Bisson as well as those from the literature plot on or close to the ideal 1:1 line, which corroborates this particular substitution. The position of a point along the line indicates the extent of substitution involving the octahedral site. The compositions of titanite from Mount Bisson plot as two separate groups with slight overlap. The *LREE*-rich niobian titanite of sample 7842 records a higher degree of substitution than does the titanite from other *LREE*-enriched rocks; this is consistent with the fact that the latter group of titanite samples contains little Nb. One of the tantalian–niobian titanite compositions from the literature (Clark 1974) shows a maximum extent of substitution of approximately 0.41 cations pfu. Three points fall significantly below the ideal line of substitution and represent heated and unheated Cardiff titanite, studied by Fleet & Henderson (1985). Subsequent re-analysis of the same material by Hawthorne *et al.* (1991) gave the data point just above these three points and within analytical error of the model line.

A portion of substitution (iii) is represented by Figure 3b (Ca *versus* *LREE* + Y + Na + Mn + Mg). The apparent increase in scatter, relative to the previous graph, reflects the change in scale as shown by the 2σ error bars. Figure 3b shows that the Mount Bisson compositions are evenly distributed about the model 1:1 line. Although they show more scatter, the titanite compositions from the literature also are uniformly distributed about the model line. The scatter probably reflects the variable quality and completeness of analytical data in the literature. For both the Mount Bisson titanite and titanite from the literature, Na occurs in small quantities; it is at or below detection in most titanite from Mount Bisson (Table 4). Sodium is commonly not sought in most of the titanite compositions reported in the literature. This makes it difficult to accurately determine the extent to which Na facilitates *LREE* substitutions at the *X* (Ca) site. The compositions of Mount Bisson titanite suggest that the amount of Na is insufficient to balance trivalent *LREE* and Y.

Figure 3c portrays the effects of the combination of mechanisms (i) and (iii). The insets repeat the compositional data of Figures 3a and 3b but in figures drawn

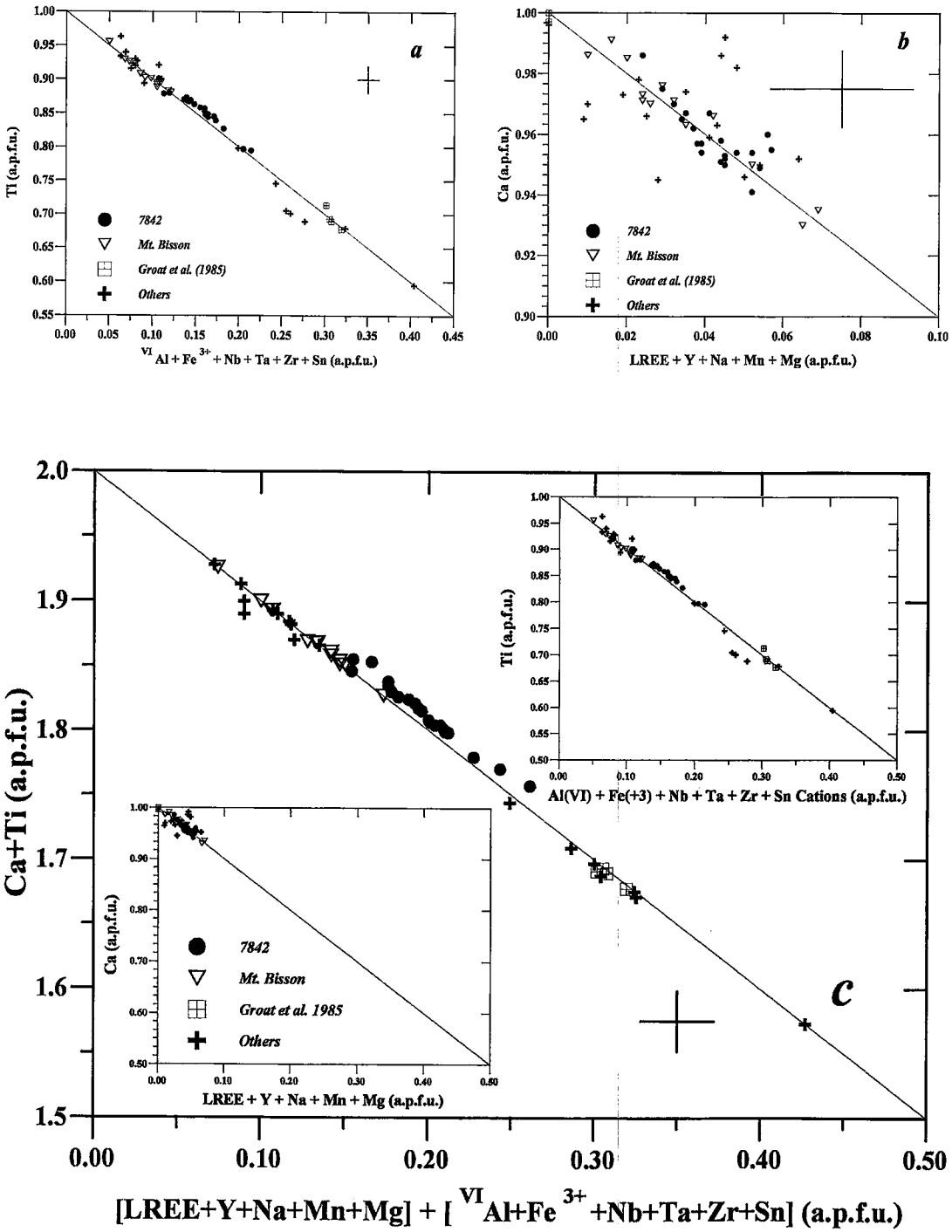

FIG. 3. a. Titanite solid-solutions are represented in terms of proportions of Ti *versus* ^{VI}Al + Fe^{3+} + Nb + Ta + Zr + Sn atoms per formula unit (apfu). Data pertain to titanite from Mount Bisson and niobium–tantalum-bearing titanite from the literature (see text). b. Compositions (as in Fig. 3a) are plotted in terms of proportions of Ca *versus* Σ*LREE* + Y + Na + Mn + Mg apfu. c. Compositions are plotted in terms of proportion Ca + Ti cations *versus* combined cationic substitutions. Insets show scaled plots of Figs. 3a and 3b.

to the same scale as Figure 3c. This combination explains the data and demonstrates that both substitutions are important in titanite from a variety of natural environments.

All three mechanisms of substitution advanced above (i, ii and iii) involve replacing Ti at the octahedral site with a trivalent cation ($^{VI}Al + Fe^{3+}$). Thus it should be possible to determine the relative importance of each of the three mechanisms in a particular case by plotting the components of each substitution against ($^{VI}Al + Fe^{3+}$). Figures 4a, 4b and 4c do this graphically for both sets of Mount Bisson data as well as for compositions from the literature. Substitution (i) is represented in Figure 4a by the solid line with a slope of 1. Compared against the analytical uncertainties (2σ error bars), only one sample of tantalian–niobian titanite (Clark 1974) has a chemical composition consistent with this substitution alone. The remainder of the titanite samples require additional substitutions to explain the observed ($^{VI}Al + Fe^{3+}$) contents.

The solid line with unit slope in Figure 4b represents a combination of substitution mechanisms (i) and (iii). Data from the literature show two types of behavior. The Nb–Ta-bearing compositions have not moved with respect to their positions in Figure 4a because they have no appreciable *LREE* or Y, and substitution (iii) is therefore not active. This includes those from Groat *et al.* (1985), which appear to be devoid of *LREE*. However, a group of the titanite compositions from the literature has shifted systematically closer to the model line, indicating that a component of these solid solutions is represented by mechanism (iii). Both sets of Mount Bisson compositions have moved closer to the 1:1 line, and some of the *LREE*-rich niobian titanite compositions of 7842 are, within analytical error, fully consistent with these two mechanisms of substitution.

The other mechanism of substitution, (ii), in combination with mechanisms (i) and (iii), is represented by a solid line with unit slope in Figure 4c. Mechanism (ii) is represented by the anions $[OH, F]^-$, which are calculated by charge balance. Most compositions plotted in Figure 4c are distributed evenly along the

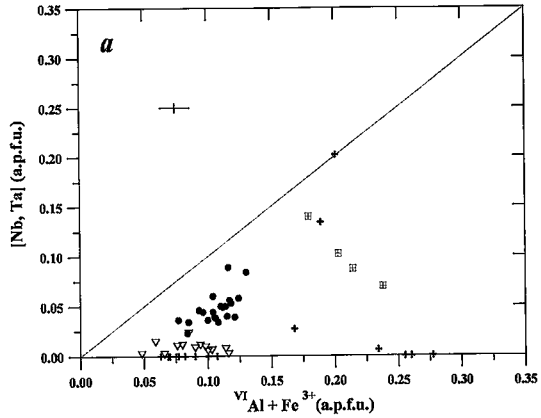

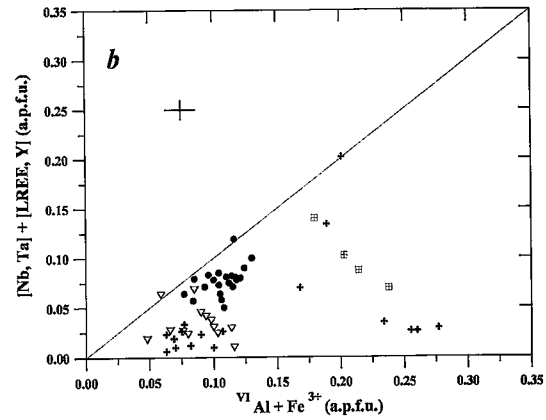

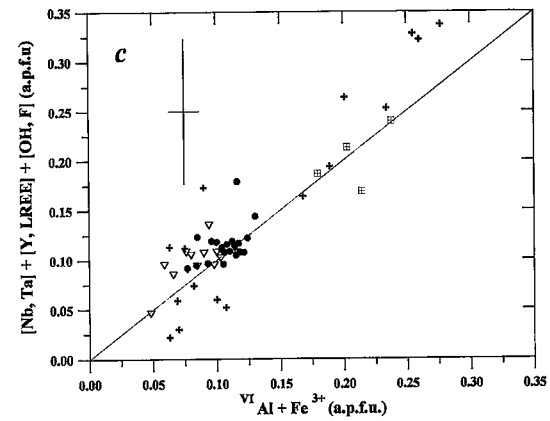

FIG. 4. a. Titanite compositions are plotted as $[Nb^{5+}, Ta^{5+}]$ *versus* $[^{VI}Al, Fe^{3+}]$; straight line with unit slope represents the exchange (i) $[Nb^{5+}, Ta^{5+}] + [^{VI}Al , Fe^{3+}] \rightleftharpoons 2Ti^{4+}$. b. Titanite samples of Fig. 4a are plotted as $[Nb^{5+}, Ta^{5+}] + [LREE, Y]^{3+}$ *versus* $[^{VI}Al, Fe^{3+}]$. Line with unit slope represents combined exchanges (i) and (iii) $[LREE, Y]^{3+} + [^{VI}Al , Fe^{3+}] \rightleftharpoons Ti^{4+} + Ca^{2+}$. c. Titanite compositions plotted as cations $[Nb^{5+}, Ta^{5+}] + [LREE, Y]^{3+}$ + calculated $[OH, F]^-$ *versus* $[^{VI}Al, Fe^{3+}]$, where a unit slope accommodates the previous two exchanges as well as (ii) $[^{VI}Al , Fe^{3+}] + (OH, F)^- \rightleftharpoons Ti^{4+} + O^{2-}$.

model line and are consistent (within analytical error) with these mechanisms of substitution. Points above the line generally have too much calculated OH^-; this can be attributed in some cases to an overestimation of trivalent cations in the octahedral site. The effect of reducing the proportion of ($^{VI}Al,Fe^{3+}$) would be to move the points both down (less calculated [OH^-, F]) and to the left. Points below the line represent samples in which Ta, Nb, Y, *LREE* or [OH^-, F] are underestimated or were not sought. The three extreme high points represent the chemical data reported by Fleet & Henderson (1985). The re-analysis of this same titanite (Hawthorne *et al.* 1991) is represented by the datum (cross) with the next highest ($^{VI}Al,Fe^{3+}$) and is well within 2σ error of the ideal line. Figures 4a, 4b and 4c show that examples of all three mechanisms of substitution are found in natural titanite, and that at least two of the three are active in almost all titanite samples.

Rare-Earth-Element Patterns

Titanite is important in the distribution of rare-earth elements in a wide variety of geochemical processes because it is one of the more pervasive accessory phases and is capable of accommodating significant quantities of the light rare-earth elements (*e.g.*, Henderson 1980, Burt 1989). In this study, we have collected a significant number of *LREE*-rich titanite compositions, which can be used to complement the existing literature on *REE* behavior in titanite-bearing systems. Chondrite-normalized concentrations of rare-earth elements [REE_{cn}] are presented in Figure 5. The data include three complete patterns with strong similarities (Henderson 1980, Gromet & Silver 1983), a set of four consistent partial patterns (Hawthorne *et al.* 1991), and the partial patterns of Giere (1986), which seem anomalous if compared to the remainder of the data set. Nakada's (1991) patterns for titanite from dacitic rocks are interesting as they record a La–Ce trend opposite to that previously reported (*e.g.*, Grauch 1989).

The Mount Bisson data-set elucidates the *LREE* behavior in titanite from igneous and metasomatic rocks. The levels of enrichment in light rare-earth elements found in titanite from the allanite-bearing granitic pegmatite (7842) (solid dots) are displayed in Figure 6a, which also shows the full REE_{cn} pattern for the host pegmatite. The titanite data in Figure 6a include rim, interior and core compositions of a variety of grains. The titanite is *LREE*-enriched relative to the bulk rock, except for La. Other *REE*-bearing accessory phases in sample 7842 include allanite, apatite, thorite, and zircon.

Profiles of *LREE*-rich titanite from other rock-types at Mount Bisson are shown in Figures 6b and 6c. REE_{cn} distributions for both alkaline (A) and subalkaline (S) intrusive rocks are shown in Figure 6b, with the partial REE_{cn} patterns for the respective titanite. The compositions of the titanite from both rock suites present broadly similar patterns; however, titanite from the alkaline rocks shows much stronger fractionation trends between La and Pr than do the subalkaline intrusive rocks. Figure 6c is the corresponding REE_{cn} plot for the Mount Bisson fenites and the partial patterns for compositions of associated titanite. The

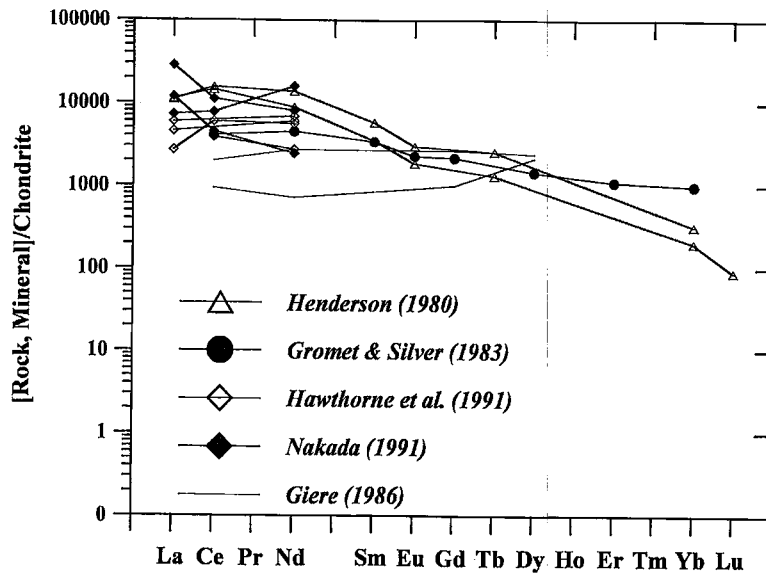

FIG. 5. Chondrite-normalized concentrations of the rare-earth elements [REE_{cn}] in titanite, taken from the literature.

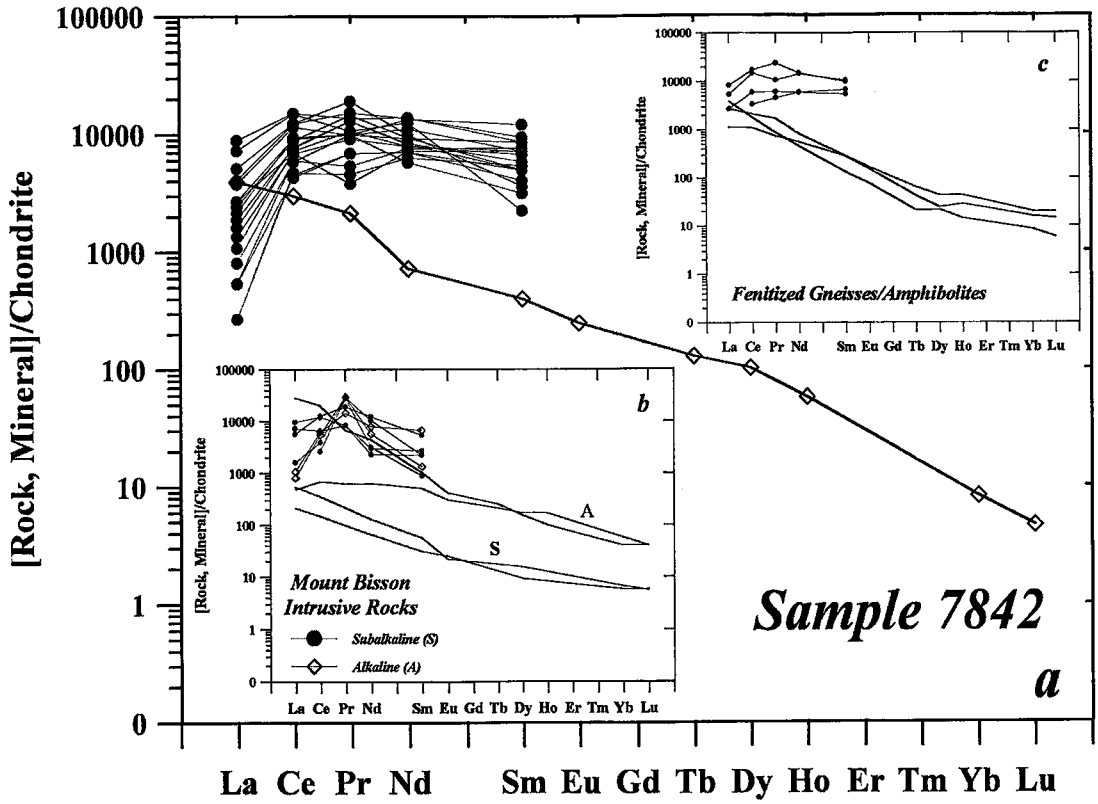

FIG. 6. a. REE_{cn} patterns for allanite-bearing granitic pegmatite 7842 and partial patterns for titanite from the same sample. b. Chemical data for Mount Bisson alkaline and subalkaline intrusive rocks and associated titanite are plotted as REE_{cn} plots. c. REE_{cn} plots for fenites, representing metasomatized metamorphic and igneous rocks, and partial patterns for compositions of associated titanite.

protoliths of these fenites include metamorphic and igneous rocks, and the titanite results from or has been influenced by *LREE*-rich metasomatic fluids. The REE_{cn} patterns for the fenites and the partial patterns for titanite show little variation despite the range of protolith compositions. The rocks are less *LREE*-enriched than the titanite grains they contain, and the $LREE_{cn}$ patterns for titanite from these metasomatically modified rocks are consistent; the patterns are relatively flat, with La showing somewhat less enrichment relative to Ce–Sm.

In summary, titanite from across the entire suite of Mount Bisson rocks (Figs. 5, 6a, b, c) show similar magnitudes of *LREE* enrichment and subtle variations in $LREE_{cn}$ patterns. These subtle variations in REE_{cn} patterns are important; whereas the degree of *LREE* enrichment in titanite mainly reflects the total *REE* content of the rock, the patterns reflect the nature of coexisting *REE*-bearing accessory phases and their sequence of crystallization. Our analysis suggests that titanite compositions in rocks containing significant allanite, apatite or zircon (Table 1) show much stronger fractionation between La and Pr. Contrast, for example, the steep positive [La–Ce] trends for titanite from the alkaline intrusive rocks, which contain significant allanite and apatite, to the much flatter trends for titanite from the subalkaline intrusions, which have little or no allanite. Similarly, the fenites generally show flatter $LREE_{cn}$ patterns than do the alkaline intrusive rocks; in the fenites, allanite is volumetrically subordinate to titanite in these rocks.

Much of the titanite found in Mount Bisson rocks shows strong compositional zoning. In the allanite-bearing granitic pegmatite (7842), however, apparent core-to-rim variations were found to be neither consistent nor to vary systematically. Some grains are characterized by a rim with high concentrations of *LREE* and Nb, relative to grain interiors, whereas other

grains in the same rock have a rim with lower *LREE* and Nb concentrations. Still other grains have low concentrations of *LREE* correlating with higher concentrations of Nb. Figure 7 shows the $LREE_{cn}$ patterns for core, interior and rim of four grains from the sample 7842. The reproducibility of these data is demonstrated in the upper left inset, where a single point on the rim of the grain was measured twice. In general, the individual grains of titanite exhibit similar patterns: moderate to weak fractionation among La, Ce and Pr, and no fractionation between Pr and Sm. It is evident in Figure 7, however, that these individual grains show no strong systematic variation in patterns between rim and core. Nor are there significant differences in degrees of *LREE* enrichment between rim and core. The best that can be stated is that the cores show the greatest degree of fractionation between La and Ce, whereas rims generally have the flattest patterns. The consistency seen in the degree of *LREE*-enrichment and the $LREE_{cn}$ patterns (Fig. 7) will facilitate evaluations of *REE* distribution patterns in rocks and interpretations of bulk-rock *REE* data in general. The apparently nonsystematic variations within individual grains of titanite may result from the superposition of a *LREE*-enriched metasomatic imprint upon original igneous titanite (*e.g.*, Jamtveit 1991) or they may reflect patterns of compositional zoning that are kinetically controlled (*cf.* Paterson & Stephens 1992).

Conclusions

Titanite from a diverse group of igneous and metasomatic rocks at Mount Bisson is enriched in *LREE* and Y. A single allanite-bearing granitic pegmatite contains *LREE*-enriched niobian titanite, which contrasts with other titanite at Mount Bisson in that Nb is greater than the combined proportions of *LREE* and Y. Such LREE-rich niobian titanite has intermediate Nb contents in relation to previously published data on Nb–Ta titanite, but has no detectable Ta.

The combination of new analytical data for *LREE*-rich niobian titanite from Mount Bisson and the data for niobian titanite from the literature suggests several mechanisms of substitution for the accommodation of significant amounts of pentavalent (Nb, Ta) and trivalent (*LREE*, Y) cations. Three dominant mechanisms appear to explain all compositions of titanite. As previously documented by Clark (1974), Paul *et al.* (1981) and Groat *et al.* (1985), much of the Nb–Ta substitution for Ti is balanced by ^{VI}Al and Fe^{3+}:

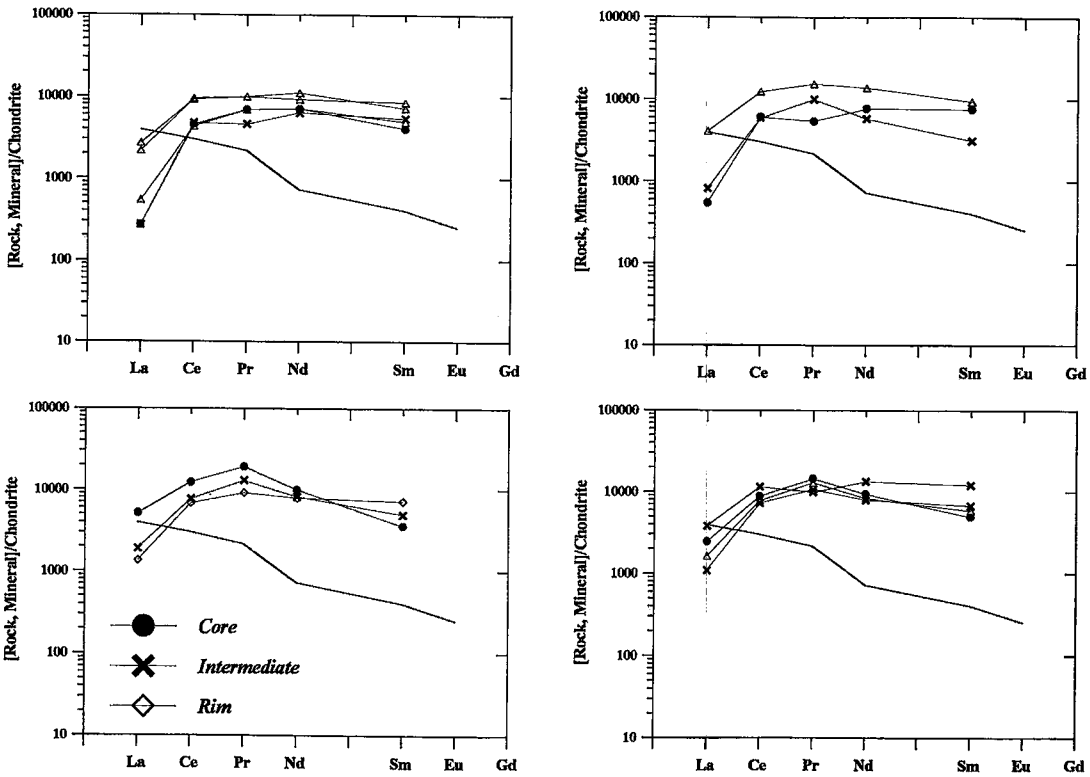

FIG. 7. Core – rim compositional variations in four grains of titanite from sample 7842 are plotted as partial REE_{cn} patterns.

(i) $[Nb, Ta]^{5+} + [^{VI}Al, Fe^{3+}] \rightleftharpoons 2Ti^{4+}$.

For most cases, including titanite from Mount Bisson rocks, this exchange (Fig. 4a) does not account for all of the observed $^{VI}Al + Fe^{3+}$. Generally, there is more than enough $^{VI}Al + Fe^{3+}$ in even the most Nb–Ta-rich titanite to accommodate the pentavalent cations. Consideration of the substitution:

(iii) $[LREE, Y]^{3+} + [^{VI}Al, Fe^{3+}] \rightleftharpoons Ti^{4+} + Ca^{2+}$

explains significantly more of the observed $^{VI}Al + Fe^{3+}$. The *LREE*-enriched niobian titanite from Mount Bisson is more completely described by these two substitutions than the corresponding simpler *LREE*-enriched titanite (Fig. 4b). Finally, consideration of $(OH,F)^{-}$-for-O substitution through the exchange:

(ii) $[^{VI}Al, Fe^{3+}] + (OH)^{-} \rightleftharpoons Ti^{4+} + O^{2-}$

(Paul *et al.* 1981, Groat *et al.* 1985) appears to account completely (within analytical error) for the observed $^{VI}Al + Fe^{3+}$ (Fig. 4c).

Titanite preferentially accommodates the *LREE* over the *HREE*; this fact, combined with its widespread occurrence as an accessory phase, make it an important mineral in terms of interpreting whole-rock REE_{cn} patterns. Within this context, the Mount Bisson data set provides a clear picture of *LREE* behavior in titanite occurring in alkaline and subalkaline igneous rocks, as well as fenites resulting from extensive metasomatism. Somewhat surprisingly, titanite from different rock-types show similar magnitudes of REE enrichment. The $LREE_{cn}$ patterns, however, record subtle but important variations. Titanite originating from more alkaline systems (*e.g.*, fenites or intrusive rocks) are characterized by moderate to high negative values of [Ce/La], whereas preliminary data from the subalkaline intrusions suggest values of $[Ce/La]_{cn}$ near zero. In contrast, Nakada's (1991) data on titanite from dacitic volcanic rocks show high positive to zero values. These differences in patterns probably reflect the presence or absence of other *REE*-rich accessory phases (*e.g.*, Exley 1980, Gromet & Silver 1983, Sawka *et al.* 1984, Halleran 1991) rather than the *REE* content of the system.

Acknowledgements

This study was supported by NSERC research grants to JKR and LAG. The University of British Columbia electron-microprobe laboratory is supported by NSERC Infrastructure grant 9924. Field work was supported by a grant from the British Columbia Department of Energy, Mines and Petroleum Resources. The manuscript benefitted from reviews and comments from R.F. Martin, Roger Mason and two anonymous reviewers.

References

Burt, D.M. (1989): Compositional and phase relations among rare earth element minerals. *In* Geochemistry and Mineralogy of Rare Earth Elements (B.R. Lipin & G.A. McKay, eds.). *Rev. Mineral.* **21**, 259-307.

Clark, A.M. (1974): A tantalum-rich variety of sphene. *Mineral. Mag.* **39**, 605-607.

Deville, E. & Struik, L.C. (1990): Polyphase tectonic, metamorphic, and magmatic events in the Wolverine Complex, Mount MacKinnon, central British Columbia. *Geol. Surv. Can., Pap.* **90-1E**, 65-69.

Drake, M.D. & Weill, D.F. (1972): New rare earth element standards for electron microprobe analysis. *Chem. Geol.* **10**, 179-181.

Exley, R.A. (1980): Microprobe studies of *REE*-rich accessory minerals: implications for Skye Granite petrogenesis and *REE* mobility in hydrothermal systems. *Earth Planet. Sci. Lett.* **48**, 97-110.

Ferri, F. & Melville, D.M. (1988): Manson Creek mapping project. *British Columbia Ministry Energy Mines & Petrol. Resources, Pap.* **1988-1**, 169-180.

_____ & _____ (1989): Geology of the Germanson Landing area, British Columbia (93N/10,15). *British Columbia Ministry Energy Mines & Petrol. Resources, Pap.* **1989-1**, 209-220.

Fleet, M.E. & Henderson, G.S. (1985): Radiation damage in natural titanite by crystal structure analysis. *Materials Res. Soc., Symp. Proc.* **50**, 363-370.

Gieré, R. (1986): Zirconolite, allanite and hoegbomite in a marble skarn from the Bergell contact aureole: implications for mobility of Ti, Zr, and *REE*. *Contrib. Mineral. Petrol.* **93**, 459-470.

Grauch, R.I. (1989): Rare earth elements in metamorphic rocks. *In* Geochemistry and Mineralogy of Rare Earth Elements (B.R. Lipin & G.A. McKay, eds.). *Rev. Mineral.* **21**, 147-167.

Groat, L.A., Carter, R.T., Hawthorne, F.C. & Ercit, T.S. (1985): Tantalian niobian titanite from the Irgon Claim, southeastern Manitoba. *Can. Mineral.* **23**, 569-571.

Gromet, L.P. & Silver, L.T. (1983): Rare earth element distributions among minerals in a granodiorite and their petrogenetic implications. *Geochim. Cosmochim. Acta* **47**, 925-939.

Halleran, A.A.D. (1991): *Geology, Geochemistry and Origins of the Mount Bisson Alkaline Rocks, Munroe Creek, British Columbia.* M.Sc. thesis, Univ. British Columbia, Vancouver, British Columbia.

———— & RUSSELL, J.K. (1990): Geology and descriptive petrology of the Mount Bisson alkaline complex, Munroe Creek, British Columbia. *British Columbia Min. Energy Mines & Petrol. Resources, Pap.* **1990-1**, 297-304.

———— & ———— (1993): Rare-earth element bearing pegmatites in the Wolverine metamorphic complex: a new exploration target. *British Columbia Min. Energy Mines & Petrol. Resources, Pap* **1993-1**, 301-306.

HAWTHORNE, F.C., GROAT, L.A., RAUDSEPP, M., BALL, N.A., KIMATA, M., SPIKE, F.D., GABA, R., HALDEN, N.M., LUMPKIN, G.R., EWING, R.C., GREEGOR, R.B., LYTLE, F.W., ERCIT, T.S., ROSSMAN, G.R., WICKS, F.J., RAMIK, R.A., SHERRIFF, B.L., FLEET, M.E. & MCCAMMON, C. (1991): Alpha-decay damage in titanite. *Am. Mineral.* **76**, 370-396.

HENDERSON, P. (1980): Rare earth element partition between sphene, apatite and other coexisting minerals of the Kangerdlugssuaq intrusion, E. Greenland. *Contrib. Mineral. Petrol.* **72**, 81-85.

JAMTVEIT, B. (1991): Oscillatory zonation patterns in hydrothermal grossular–andradite garnet: nonlinear dynamics in regions of immiscibility. *Am. Mineral.* **76**, 1319-1327.

KRETZ, R. (1983): Symbols for rock-forming minerals. *Am. Mineral.* **68**, 277-279.

MADER, U.K., THIRUGNANAM, U. & RUSSELL, J.K. (1988): *Formula-A: a Turbo-PASCAL Program for the Calculation of Mineral Structural Formulae.* The University of British Columbia, unpublished software documentation.

MANSY, J.L. & GABRIELSE, H. (1978): Stratigraphy, terminology and correlation of Upper Proterozoic rocks in Omineca and Cassiar Mountains, north-central British Columbia. *Geol. Surv. Can., Pap.* **77-19**.

MONGIORGI, R. & RIVA DE SANSEVERINO, L. (1968): A reconsideration of the structure of titanite, $CaTiOSiO_4$. *Mineral. Petrogr. Acta* **14**, 123-141.

NAKADA, S. (1991): Magmatic processes in titanite-bearing dacites, central Andes of Chile and Bolivia. *Am. Mineral.* **76**, 548-560.

PARRISH, R.R. (1979): Geochronology and tectonics of the Northern Wolverine Complex, British Columbia. *Can. J. Earth Sci.* **16**, 1428-1438.

PATERSON, B.A. & STEPHENS, W.E. (1992): Kinetically induced compositional zoning in titanite: implications for accessory-phase/melt partitioning of trace elements. *Contrib. Mineral. Petrol.* **109**, 373-385.

PAUL, B.J., ČERNÝ, P. & CHAPMAN, R. (1981): Niobian titanite from the Huron Claim Pegmatite, southeastern Manitoba. *Can. Mineral.* **19**, 549-552.

SAWKA, W.N., CHAPPELL, B.W. & NORRISH, K. (1984): Light-rare-earth-element zoning in sphene and allanite during granitoid fractionation. *Geology* **12**, 131-134.

TIPPER, H.W., CAMPBELL, R.B., TAYLOR, G.C. & STOTT, D.F. (1974): Parsnip River, British Columbia. *Geol. Surv. Can., Map* **142A**, *Sheet* **93**.

ZACHARIASEN, W.H. (1930): The crystal structure of titanite. *Z. Kristallogr.* **73**, 7-16.

Received February 9, 1993, revised manuscript accepted January 23, 1994.